



U.S. Department
of Transportation
**National Highway
Traffic Safety
Administration**



DOT HS 813 086

February 2022

Comparison of the aPLI, FlexPLI With Upper Body Mass, and FlexPLI Pedestrian Legforms in Matched-Pair Vehicle Tests

DISCLAIMER

This publication is distributed by the U.S. Department of Transportation, National Highway Traffic Safety Administration, in the interest of information exchange. The opinions, findings and conclusions expressed in this publication are those of the authors and not necessarily those of the Department of Transportation or the National Highway Traffic Safety Administration. The United States Government assumes no liability for its contents or use thereof. If trade or manufacturers' names are mentioned, it is only because they are considered essential to the object of the publication and should not be construed as an endorsement. The United States Government does not endorse products or manufacturers.

NOTE: This report is published in the interest of advancing motor vehicle safety research. While the report may provide results from research or tests using specifically identified motor vehicle models, it is not intended to make conclusions about the safety performance or safety compliance of those motor vehicles, and no such conclusions should be drawn.

Suggested APA Format Citation:

Suntay, B., & Stammen, J. (2022, February). *Comparison of the aPLI, FlexPLI with upper body mass, and FlexPLI pedestrian legforms in matched-pair vehicle tests* (Report No. DOT HS 813 086). National Highway Traffic Safety Administration.

1. Report No. DOT HS 813 086		2. Government Accession No.		3. Recipient's Catalog No.	
4. Title and Subtitle Comparison of the aPLI, FlexPLI With Upper Body Mass, and FlexPLI Pedestrian Legforms in Matched-Pair Vehicle Tests				5. Report Date February 2022	
				6. Performing Organization Code	
7. Authors Brian Suntay, Transportation Research Center Inc. and Jason Stammen, NHTSA Vehicle Research and Test Center				8. Performing Organization Report No.	
9. Performing Organization Name and Address Transportation Research Center Inc. and Vehicle Research and Test Center 10820 OH-347 East Liberty, OH 43319				10. Work Unit No. (TRAIS)	
				11. Contract or Grant No.	
12. Sponsoring Agency Name and Address National Highway Traffic Safety Administration 1200 New Jersey Avenue SE Washington, DC 20590				13. Type of Report and Period Covered Final Report	
				14. Sponsoring Agency Code	
15. Supplementary Notes					
16. Abstract Pedestrian knee ligament injuries and lower leg fractures are the most frequent and among the most debilitating long-term injuries in motor vehicle crashes. Global Technical Regulation No. 9, Pedestrian Safety, has been adopted by the international community to mitigate these pedestrian injuries through improved vehicle bumper systems. The current UN GTR includes the flexible pedestrian legform impactor (FlexPLI), which simulates the lower limb of a pedestrian and is the device widely used in global New Car Assessment Programs to assess the protection level of the front-end structures of vehicles. The objective of this study was to perform a preliminary evaluation of the upper body part addition to the FlexPLI (FlexPLI-UBM) and the advanced pedestrian legform impactor. Test results from the advanced legforms used in this evaluation were compared to each other and to the current FlexPLI at matched impact locations.					
17. Key Words FlexPLI, FlexPLI-UBM, NCAP, UN GTR, aPLI, UBM, VRTC				18. Distribution Statement Document is available to the public from the National Technical Information Service, www.ntis.gov .	
19. Security Classif. (of this report) Unclassified		20. Security Classif. (of this page) Unclassified		21. No. of Pages 36	22. Price

Form DOT F 1700.7 (8-72)

Reproduction of completed page authorized

Table of Contents

1. Introduction	1
2. Objective	3
3. Overview of Legform Impactors	4
3.1. FlexPLI-UBM (FlexPLI With Upper Body Mass)	4
3.2. Advanced Pedestrian Legform Impactor, aPLI	5
4. Vehicle and Test Setup	9
4.1. FlexPLI-UBM Test Setup	10
4.2. The aPLI Test Setup.....	12
5. Results	13
5.1. Center Impact Results	13
5.2. Outboard Impact Results.....	17
6. Summary	22
7. Discussion	23
8. Limitations	26
9. Conclusion	27
10. References	28

List of Figures

Figure 1. The FlexPLI-UBM upper body part: (Top Left) Lateral/struck-side view with the black flexible rubber element and base plate shown; (Bottom Left) Anterior-lateral oblique view; (Right) Anterior view as mounted on the standard FlexPLI legform.	4
Figure 2. The FlexPLI and aPLI shown side-by side: (Left) Anterior view; (Right) Lateral/struck-side view. In both views, the FlexPLI is shown on the left and the aPLI is shown on the right. ...	5
Figure 3. View of the SUBP: (Left) Anterior view; (Right) Lateral/struck-side view.	6
Figure 4. A view of the aPLI next to its one-piece molded flesh system.	6
Figure 5. The legform depth/thickness along the femur increases towards the SUBP (Left) while the depth/thickness along the tibia increases towards the knee (Right), creating a more contoured contact surface in the aPLI, as shown by the red line.	7
Figure 6. Rounded knee block of the aPLI to improve legform response in oblique impacts.....	7
Figure 7. Knee ligament orientation in the human (Left) versus the FlexPLI (Middle) and aPLI (Right).	8
Figure 8. Oblique view of the 2016 Ford Edge.	9
Figure 9. Frontal view of the 2016 Ford Edge shown with legform impact locations.	10
Figure 10. Additional support pieces were added to the existing VRTC legform launcher to support the UBM during launch.	11
Figure 11. View of the aPLI carriage attached to VRTC's launch system.	12
Figure 12. Center impact screen captures from high speed videos of the FlexPLI-UBM (Top Row), aPLI (Middle Row), and FlexPLI (Bottom Row) at time of first contact (T ₀), time of maximum bending (T _{Max}), and time of rebound (T _{Rebound}).	14
Figure 13. Femur bending moment time histories for the center impact: Femur 1 (closest to the knee) is shown at the top left; Femur 2 is at the top right; and Femur 3 (furthest from the knee) is at the bottom. The FlexPLI-UBM is shown in green (T _{max} = 0.028 s; T _{Rebound} = 0.071 s). The aPLI is shown in red (T _{max} = 0.028 s; T _{Rebound} = 0.058 s). The standard FlexPLI is shown in blue (T _{max} = 0.022 s; T _{Rebound} = 0.053 s). The grey areas indicate the regions of maximum bending and rebound, which correspond with the screen captures in Figure 12.	15
Figure 14. Ligament elongation time histories for the center impact: MCL is shown at the top left; PCL is at the top right; and ACL is at the bottom. The FlexPLI-UBM is shown in green (T _{max} = 0.028 s; T _{Rebound} = 0.071 s). The aPLI is shown in red (T _{max} = 0.028 s; T _{Rebound} = 0.058 s). The standard FlexPLI is shown in blue (T _{max} = 0.022 s; T _{Rebound} = 0.053 s). The grey areas indicate the regions of maximum bending and rebound, which correspond with the screen captures in Figure 12.	16
Figure 15. Tibia bending moment time histories for the center impact: Tibia 1 (closest to the knee) is shown at the top left; Tibia 2 is at the top right; Tibia 3 is at the bottom left; and Tibia 4 (furthest from the knee) is at the bottom right. The FlexPLI-UBM is shown in green (T _{max} = 0.028 s; T _{Rebound} = 0.071 s). The aPLI is shown in red (T _{max} = 0.028 s; T _{Rebound} = 0.058 s). The standard FlexPLI is shown in blue (T _{max} = 0.022 s; T _{Rebound} = 0.053 s). The grey areas indicate the regions of maximum bending and rebound, which correspond with the screen captures in Figure 12.	17
Figure 16. Outboard impact screen captures from high speed videos of the FlexPLI-UBM (Top Row), aPLI (Middle Row), and FlexPLI (Bottom Row) at time of first contact (T ₀), time of maximum bending (T _{Max}), and time of rebound (T _{Rebound}).	18
Figure 17. Femur bending moment time histories for the outboard impact: Femur 1 (closest to the knee) is shown at the top left; Femur 2 is at the top right; and Femur 3 (furthest from the knee) is	

at the bottom. The FlexPLI-UBM is shown in green ($T_{max} = 0.033$ s; $T_{Rebound} = 0.071$ s). The aPLI is shown in red ($T_{max} = 0.029$ s; $T_{Rebound} = 0.067$ s). The standard FlexPLI is shown in blue ($T_{max} = 0.018$ s; $T_{Rebound} = 0.055$ s). The grey areas indicate the regions of maximum bending and rebound, which correspond with the screen captures in Figure 16. 19

Figure 18. Ligament elongation time histories for the outboard impact: MCL is shown at the top left; PCL is at the top right; and ACL is at the bottom. The FlexPLI-UBM is shown in green ($T_{max} = 0.033$ s; $T_{Rebound} = 0.071$ s). The aPLI is shown in red ($T_{max} = 0.029$ s; $T_{Rebound} = 0.067$ s). The standard FlexPLI is shown in blue ($T_{max} = 0.018$ s; $T_{Rebound} = 0.055$ s). The grey areas indicate the regions of maximum bending and rebound, which correspond with the screen captures in Figure 16..... 20

Figure 19. Tibia bending moment time histories for the outboard impact: Tibia 1 (closest to the knee) is shown at the top left; Tibia 2 is at the top right; Tibia 3 is at the bottom left; and Tibia 4 (furthest from the knee) is at the bottom right. The FlexPLI-UBM is shown in green ($T_{max} = 0.033$ s; $T_{Rebound} = 0.071$ s). The aPLI is shown in red ($T_{max} = 0.029$ s; $T_{Rebound} = 0.067$ s). The standard FlexPLI is shown in blue ($T_{max} = 0.018$ s; $T_{Rebound} = 0.055$ s). The grey areas indicate the regions of maximum bending and rebound, which correspond with the screen captures in Figure 16..... 21

Figure 20. Knee centerline impact locations for the FlexPLI, FlexPLI-UBM, and aPLI. 23

Figure 21. Outboard impact screen captures from high speed videos at T_{Max} (Top Row), and $T_{Rebound}$ (Bottom Row) for the FlexPLI-UBM (left), aPLI (center), and standard FlexPLI (right). 25

List of Tables

Table 1. Test numbers, impact locations, and impact heights for each of the three legforms.....	13
Table 2. Summary of peak magnitudes for the center and outboard impacts with the three legforms	22

1. Introduction

Pedestrian knee ligament injuries and lower leg fractures are the most frequent and among the most debilitating long-term injuries in motor vehicle crashes. Global Technical Regulation¹ No. 9², Pedestrian Safety, has been adopted by the international community to mitigate these pedestrian injuries through improved vehicle bumper systems. The current UN GTR includes the flexible pedestrian legform impactor (FlexPLI), which simulates the lower limb of a pedestrian and is the device that has been widely used in global New Car Assessment Programs (NCAP) to assess the protection level of the front-end structures of vehicles. A previous study (Suntay & Stammen, 2014) evaluating the FlexPLI concluded that the lower legform test device is:

- **Durable**, as it didn't sustain any significant structural damage in 30+ vehicle bumper impacts at 40 km/h. Many of these vehicles were far from complying with the GTR injury limits.
- **Repeatable**, with percentage coefficients of variation (%CV) below 5 percent for all channels and below 2 percent for all injury channels (MCL and Tibia 1 bending moment) in vehicle bumper tests.
- **Reproducible**, with %CV below 10 percent for three different legforms in vehicle bumper tests and below 4 percent in pendulum qualification tests without vehicle or test setup-related variance.
- **Sensitive to vehicle design**, as demonstrated through testing a large range of compliant and non-compliant bumper systems. The FlexPLI discriminated between systems containing pedestrian countermeasures, such as the lower bumper stiffener and modular energy absorber, and older model year, non-GTR compliant systems present in the U.S. fleet.
- **Biofidelic**, as the knee and tibia portions of the legform maintained conformance with qualification corridors derived from biomechanical data

While the FlexPLI has better biofidelity than previous test tools and the qualities necessary to be a regulatory test device, it is not used to assess bending loads above the knee during a vehicle collision because the upper portion of the legform does not bend realistically. For many vehicles, femur bending loads are low due to the lack of an upper body mass representation that would otherwise cause the femur to wrap around the front end of the vehicle. There is currently an additional upper legform impactor test to evaluate femur and pelvis injuries used in global NCAP programs (Suntay & Stammen, May 2019). By improving the above knee biofidelity of the FlexPLI, both the upper and lower legform tests could be combined into a single legform test. Additionally, a single legform test would decrease the number of tests needed and would provide

¹ In 1998 the United Nations Economic Commission for Europe (UNECE) adopted an "Agreement concerning the Establishing of Global Technical Regulations for Wheeled Vehicles, Equipment and Parts which can be fitted and/or be used on Wheeled Vehicles," or 1998 Agreement, following its mission to harmonize vehicle regulations. It established United Nations Global Technical Regulations (UN GTRs) in a U.N. Global Registry. The UN GTRs contain globally harmonized performance requirements and test procedures. Each UN GTR text includes a record of the technical rationale, the research sources used, cost and benefit considerations, and references to data consulted. It currently has 33 contracting parties and 14 UN GTRs have been established in the UN Global Registry. Manufacturers and suppliers cannot use directly the UN GTRs as these are intended to serve the countries and require transposition in national or regional law.

² Adopted November 12, 2008.

both cost and time savings in the purchase and replacement of vehicle parts needed for evaluation.

In order to further improve the biofidelity of the FlexPLI both below and above the knee, research has been done that introduces an upper body mass to the lower legform impactor. Under the Safety Enhanced Innovations for Older Road Users (SENIORS) project, the Federal Highway Research Institute,³ and Transport Research Laboratory (TRL) developed a flexible upper body mass attachment, representing the torso of a pedestrian, that attaches to the top of the current FlexPLI (FlexPLI-UBM) to add hip rotation to the impactor kinematics and provide the time lag observed in the kinematics of human body models (Zander & Hynd, 2018). In a separate but concurrent effort, the Japan Automobile Research Institute (JARI) in conjunction with the Japan Automobile Manufacturers Association, Inc. (JAMA), also modified the mass, shape, geometry, and stiffness of the current lower legform impactor to develop the advanced pedestrian legform impactor (aPLI).

³ German name Bundesanstalt für Straßenwesen, with the acronym BASt.

2. Objective

The objective of this study was to perform a preliminary evaluation of the upper body part addition to the FlexPLI (FlexPLI-UBM) and the aPLI. Test results from the advanced legforms used in this evaluation were compared to each other and to the current FlexPLI at matched impact locations.

3. Overview of Legform Impactors

A detailed evaluation of the FlexPLI was conducted previously (Suntay & Stammen, 2014). The following sections will provide a brief overview of the updated legforms. For direct comparison purposes, the aPLI was considered to be a right leg consistent with the FlexPLI.

3.1. FlexPLI-UBM (FlexPLI With Upper Body Mass)

The upper body mass (UBM) was developed as a bolt-on attachment to the current FlexPLI. It consists of a rigid upper body part with a urethane covering to mimic the hip flesh that is attached with a flexible rubber element and base plate to the upper femur part of the FlexPLI. The UBM is shown in Figure 1.

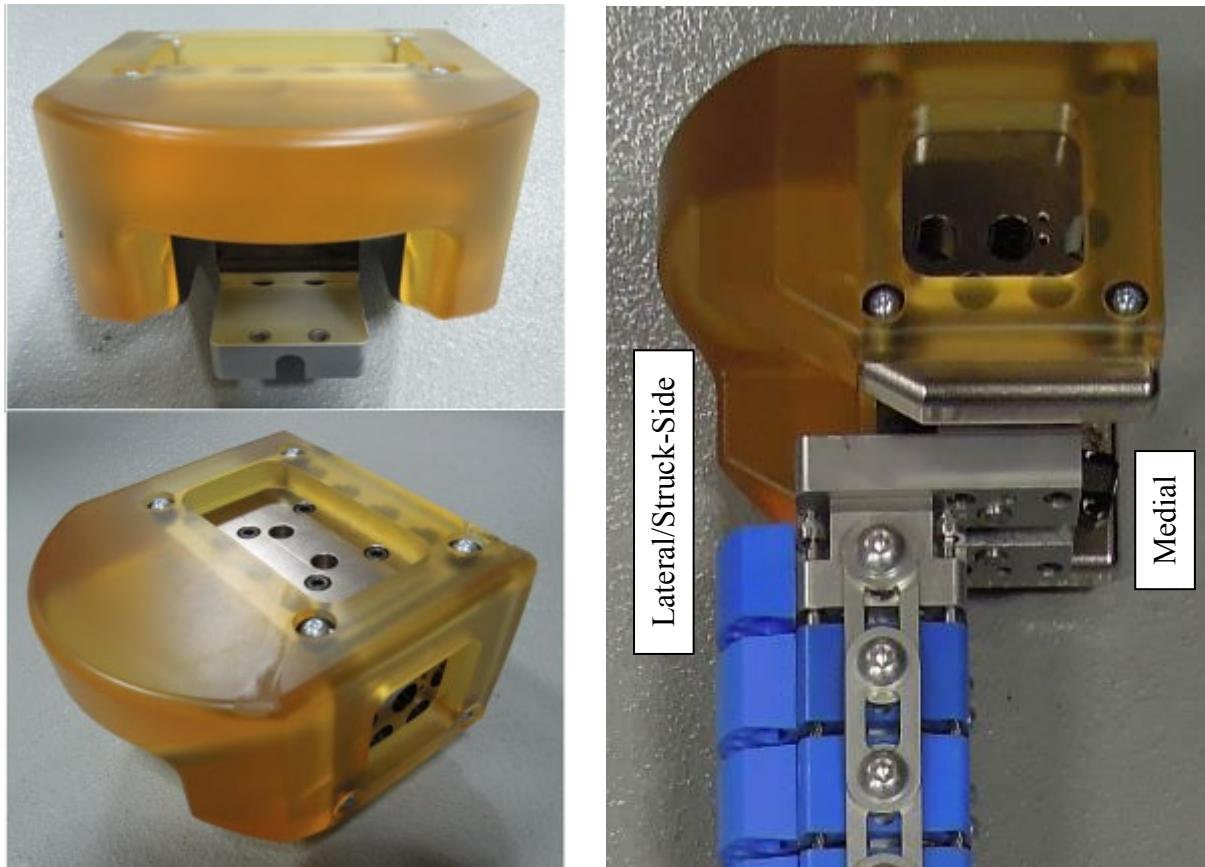


Figure 1. The FlexPLI-UBM upper body part: (Top Left) Lateral/struck-side view with the black flexible rubber element and base plate shown; (Bottom Left) Anterior-lateral oblique view; (Right) Anterior view as mounted on the standard FlexPLI legform.

The mass of the UBM is 7.0 kg, which results in a total impactor mass (FlexPLI + UBM) of 20.0 kg. FlexPLI-UBM instrumentation is the same as the FlexPLI as no instrumentation was added with the upper body part.

3.2. Advanced Pedestrian Legform Impactor, aPLI

The aPLI improves upon the FlexPLI by adding a simplified upper body part (SUBP) to represent the pelvis and upper body mass of a pedestrian and by modifying the mass distribution, geometry, and femur stiffness of the lower legform. The current FlexPLI and aPLI are pictured side-by-side in Figure 2.

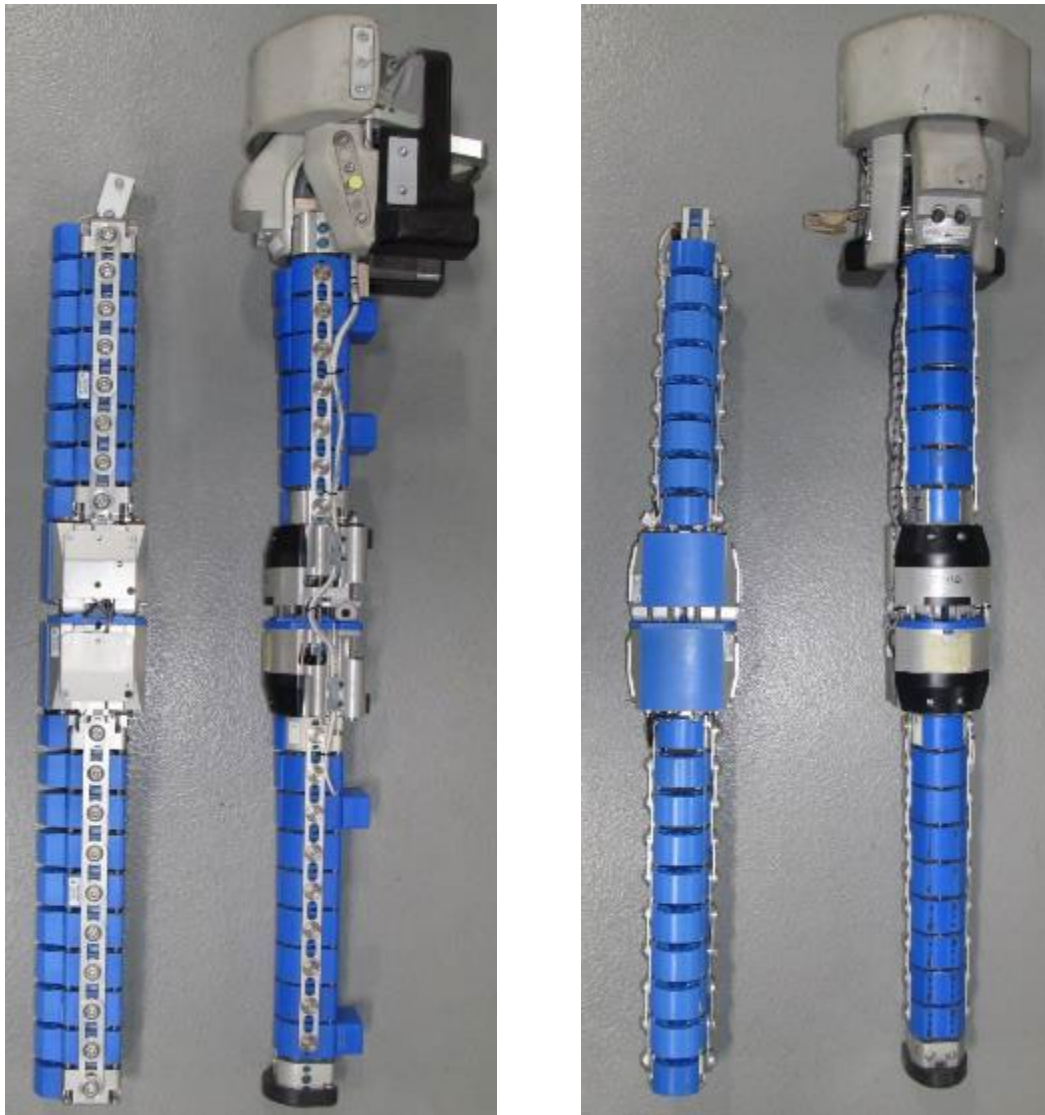


Figure 2. The FlexPLI and aPLI shown side-by-side: (Left) Anterior view; (Right) Lateral/struck-side view. In both views, the FlexPLI is shown on the left and the aPLI is shown on the right.

The mass and shape of the flesh and pelvis of the SUBP were optimized using finite element (FE) modeling in order to improve the legform's contact characteristics with a vehicle front-end and to better match human full-body FE model simulations. A closer view of the resulting SUBP of the aPLI is shown in Figure 3.



Figure 3. View of the SUBP: (Left) Anterior view; (Right) Lateral/struck-side view.

Unlike the UBM, the SUBP is not a bolt-on attachment to the current FlexPLI. The aPLI is an entirely different legform than the FlexPLI. The mass of the aPLI flesh was increased while the mass of the long bones was decreased in order to better match the mass distribution of a human leg. The stiffness of the femur was also increased to better match the stiffness of the human femur. Additionally, the black rubber sheets used to represent the flesh in the FlexPLI was replaced with a one-piece molded flesh system (Figure 4) for improved assembly repeatability.



Figure 4. A view of the aPLI next to its one-piece molded flesh system.

The legform contact geometry was modified by introducing curvatures into the shape of the impact surface of the legform to better match the shape of the human tibia and femur and improve contact response. In the FlexPLI, the contact surface is straight and the legform has uniform thickness throughout. In the aPLI, the legform depth/thickness along the femur increases towards the SUBP while the depth/thickness along the tibia increases towards the knee, creating a more contoured contact surface (Figure 5). The square knee blocks of the FlexPLI were also rounded to improve the response during oblique impacts (Figure 6).

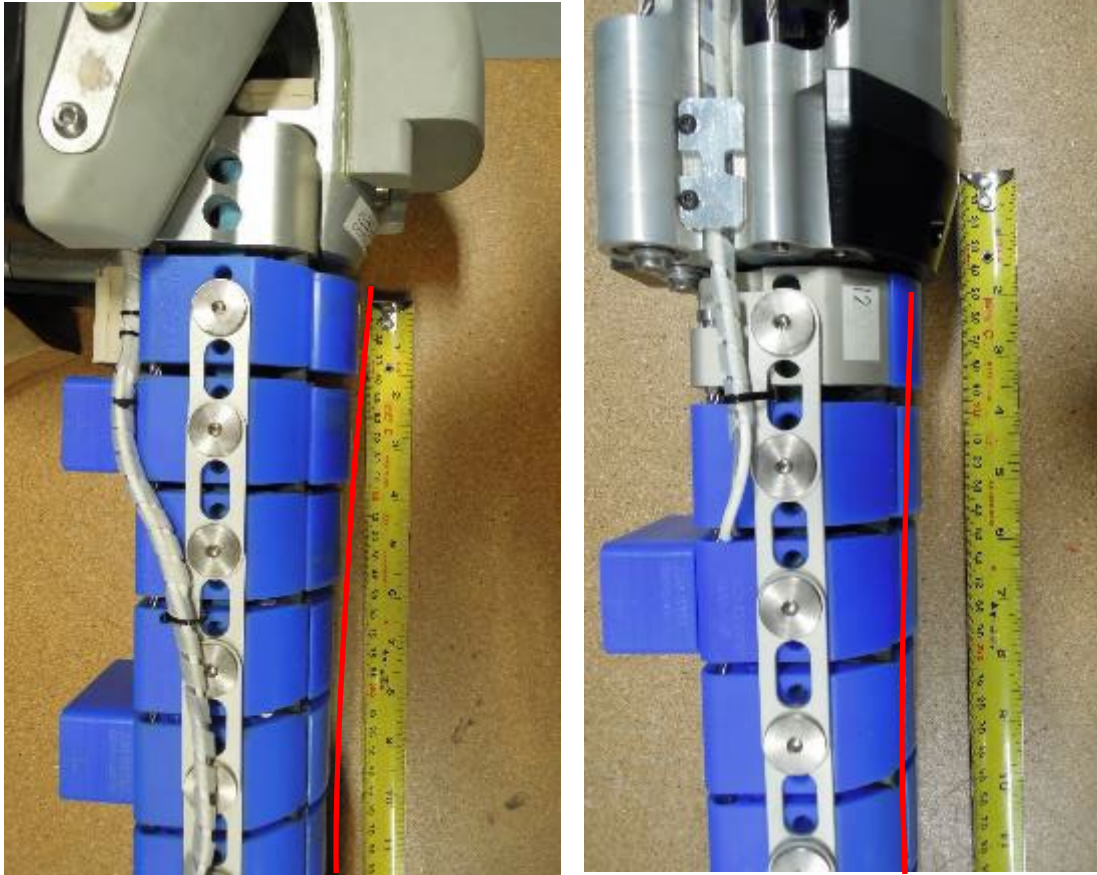


Figure 5. The legform depth/thickness along the femur increases towards the SUBP (Left) while the depth/thickness along the tibia increases towards the knee (Right), creating a more contoured contact surface in the aPLI, as shown by the red line.



Figure 6. Rounded knee block of the aPLI to improve legform response in oblique impacts. Additionally, the orientation of the knee ligaments was modified to be vertical to improve biofidelity (Figure 7).

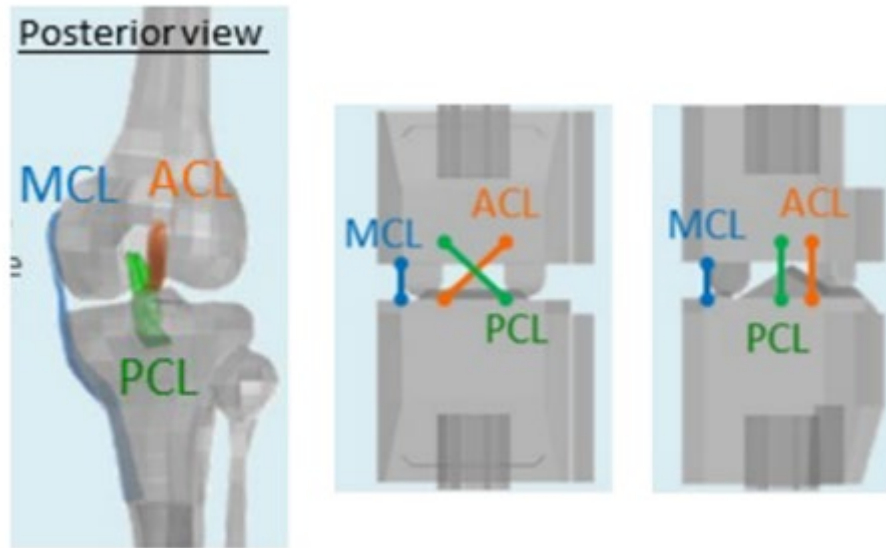


Figure 7. Knee ligament orientation in the human (Left) versus the FlexPLI (Middle) and aPLI (Right).

Similar to the FlexPLI, the aPLI has three strain gages along the femur; four strain gages along the tibia; string potentiometers that represent the medial collateral ligament (MCL), anterior cruciate ligament (ACL), and posterior cruciate ligament (PCL); and an accelerometer located at the knee.

The aPLI does not have a string potentiometer to represent the lateral collateral ligament (LCL). Because the aPLI is always struck on the lateral aspect, only the MCL is stretched.

In addition to the instrumentation that already exists in the FlexPLI, the aPLI has an added angular rate sensor at the knee, three accelerometers within the SUBP, and three angular rate sensors within the SUBP. The onboard data acquisition system was also moved to be within the SUBP instead of the knee as in the FlexPLI.

The total mass of the aPLI is 25.0 kg, which is 5.0 kg greater than the FlexPLI-UBM mass of 20.0 kg. The FlexPLI mass is 13.0 kg.



Figure 9. Frontal view of the 2016 Ford Edge shown with legform impact locations.

For all tests performed in this study, the EuroNCAP test protocol was used for vehicle preparation, vehicle mark-up, set-up, and testing with a few exceptions. First, due to the increased mass of the aPLI and UBM, the legform launcher system at NHTSA's Vehicle Research and Test Center (VRTC) in East Liberty, Ohio, was unable to stably achieve the target free flight velocity of 11.1 m/s; therefore, all tests were performed at a target speed of 9 m/s. Second, the height of the bottom of the legform to the ground reference plane at the time of impact varied between legforms. The implications of this variation between legforms will be explained in the following sections.

4.1. FlexPLI-UBM Test Setup

To launch the FlexPLI-UBM, modifications were made to VRTC's existing FlexPLI launch carriage to support the upper body part during the launch and acceleration of the legform. The additional support pieces are shown in Figure 10.

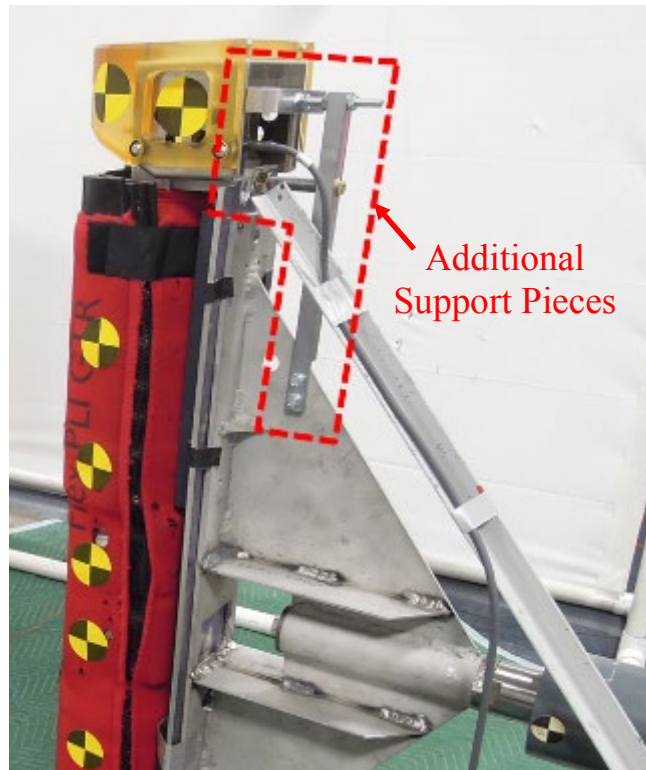


Figure 10. Additional support pieces were added to the existing VRTC legform launcher to support the UBM during launch.

During the free flight phase in speed trial tests, the FlexPLI-UBM was observed to drop 27 mm before the time of impact with a vehicle front-end. This drop was subsequently taken into account when positioning the vehicle height such that at the time of impact, the height of the bottom of the legform with respect to the vehicle's GRL was at the target test height.

The FlexPLI-UBM impact conditions were derived from the legform's geometry and its possible interactions with a vehicle front-end (Zander et al., 2019). The target height of the FlexPLI-UBM with respect to the GRL at the time of impact with a vehicle front-end varies and is defined by the vehicle bonnet leading edge (BLE) and wrap around distance (WAD). According to FlexPLI-UBM procedures, for a given BLE WAD, the distance of the bottom of the legform from the GRL shall be:

$$\begin{aligned}
 &25 \text{ mm for BLE WAD} \leq 953 \text{ mm} \\
 &(\text{BLE WAD} - 928 \text{ mm}) \text{ for } 954 \text{ mm} \leq \text{BLE WAD} \leq 1000 \text{ mm} \\
 &72 \text{ mm for BLE WAD} > 1000 \text{ mm}
 \end{aligned}$$

The 2016 Ford Edge BLE WAD was measured to be 991 mm, resulting in a legform bottom to GRL target height of 63 mm.

4.2. The aPLI Test Setup

In order to launch the aPLI, a custom launch carriage was adapted to the VRTC launch system. The aPLI launch carriage is shown in Figure 11 attached to the VRTC launch system.



Figure 11. View of the aPLI carriage attached to VRTC's launch system.

During free flight, the aPLI was observed to drop 56 mm before the time of impact with a vehicle front-end. As with the FlexPLI-UBM, this drop was subsequently taken into account when positioning the vehicle height such that at the time of impact, the height of the bottom of the aPLI with respect to the vehicle's GRL was at the target test height.

Previous human body modeling studies determined that the bottom of the foot should be 25 mm from the ground to account for shoe sole height. For the current FlexPLI, the target height of the bottom of the legform from the GRL is specified to be 75 mm. This height was increased from the original 25 mm shoe sole height because it was found that the FlexPLI, with its lack of upper body mass, better matched the response of full-body human model simulations at a higher impact height (Miyazaki et al., 2009). Since the aPLI includes an upper body mass, the target height of the bottom of the aPLI from the GRL was brought back down to 25 mm (Isshiki et al., 2018).

5. Results

Test numbers, impact locations, and impact heights are listed in Table 1.

Table 1. Test numbers, impact locations, and impact heights for each of the three legforms

Legform	Test #	Impact Location	Bottom of Legform Height wrt Ground
aPLI	1805	L+4, Passenger	25 mm
	1807	L0, Center	
FlexPLI-UBM	1901	L+4, Passenger	63 mm
	1902	L0, Center	
FlexPLI	1803	L-4, Driver	75 mm
	1804	L0, Center	

5.1. Center Impact Results

Screen captures from high speed videos of the FlexPLI-UBM, aPLI, and FlexPLI at time of first contact (T₀), time of maximum bending (T_{Max}), and time just before contact separation (T_{Rebound}) are shown in Figure 12 for the center impact. The FlexPLI-UBM, aPLI, and FlexPLI show similar impact kinematics from time of first contact through time of maximum bending. The rebound phase is where the legforms deviate from one another kinematically. Both the FlexPLI-UBM and aPLI maintain a forward pitch towards the vehicle during rebound while the FlexPLI pitches rearward and away from the vehicle.

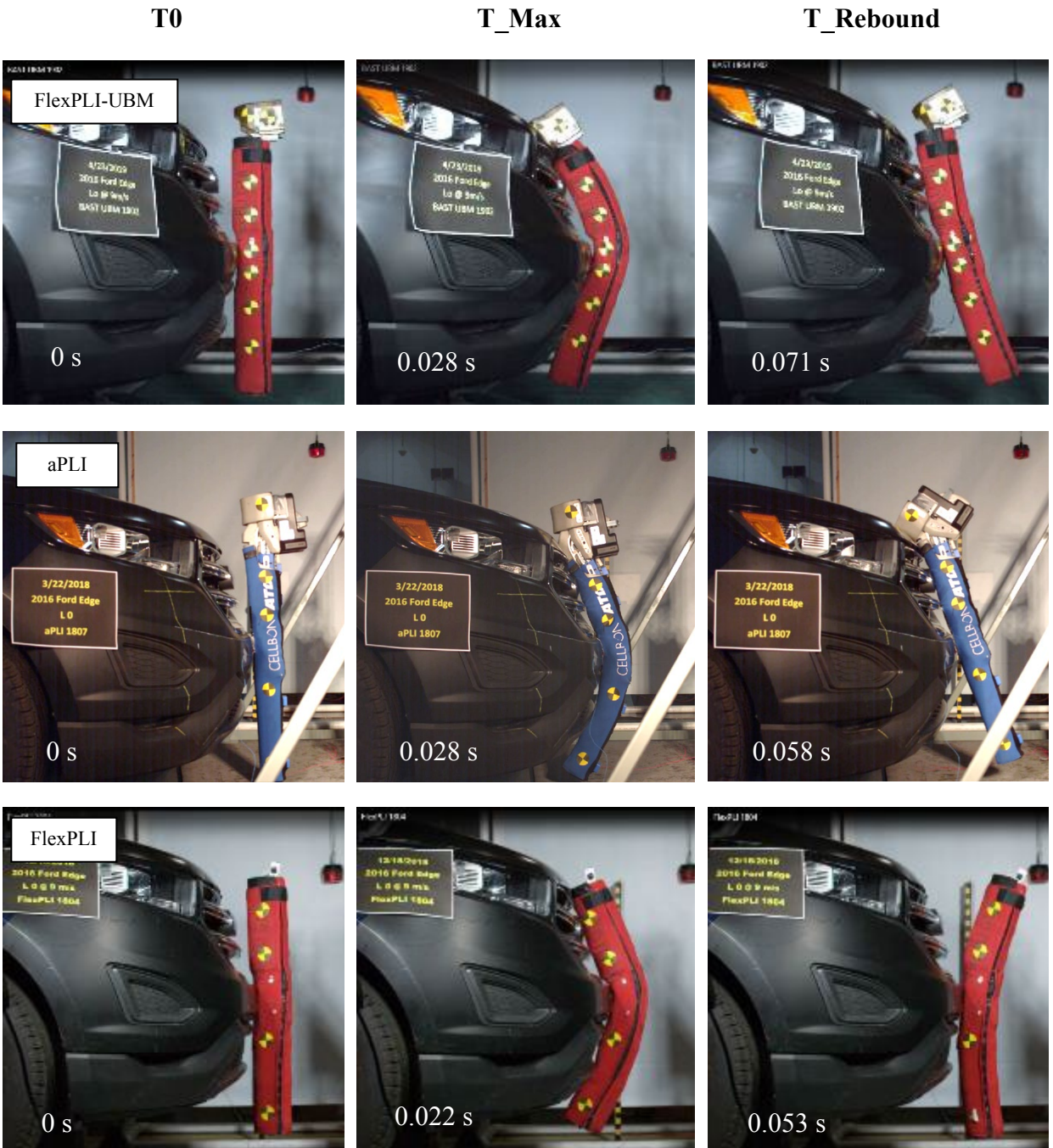


Figure 12. Center impact screen captures from high speed videos of the FlexPLI-UBM (Top Row), aPLI (Middle Row), and FlexPLI (Bottom Row) at time of first contact (T₀), time of maximum bending (T_{Max}), and time of rebound (T_{Rebound}).

Center impact time histories for femur bending moment (Figure 13), knee ligament elongation (Figure 14), and tibia bending moment (Figure 15) are shown below for the FlexPLI-UBM, aPLI, and FlexPLI. The results for the FlexPLI-UBM, aPLI, and FlexPLI are represented by the green, red, and blue curves, respectively. The results indicate that the advanced legforms exhibited greater femur bending moments and MCL/PCL elongations, lower ACL elongations, and similar tibia bending moments when compared to the standard FlexPLI. Additionally, with regard to ACL elongations, the aPLI exhibited a secondary peak after the time of maximum bending and during the rebound phase that was greater in magnitude than the first peak, but still lower in magnitude than both the FlexPLI-UBM and FlexPLI.

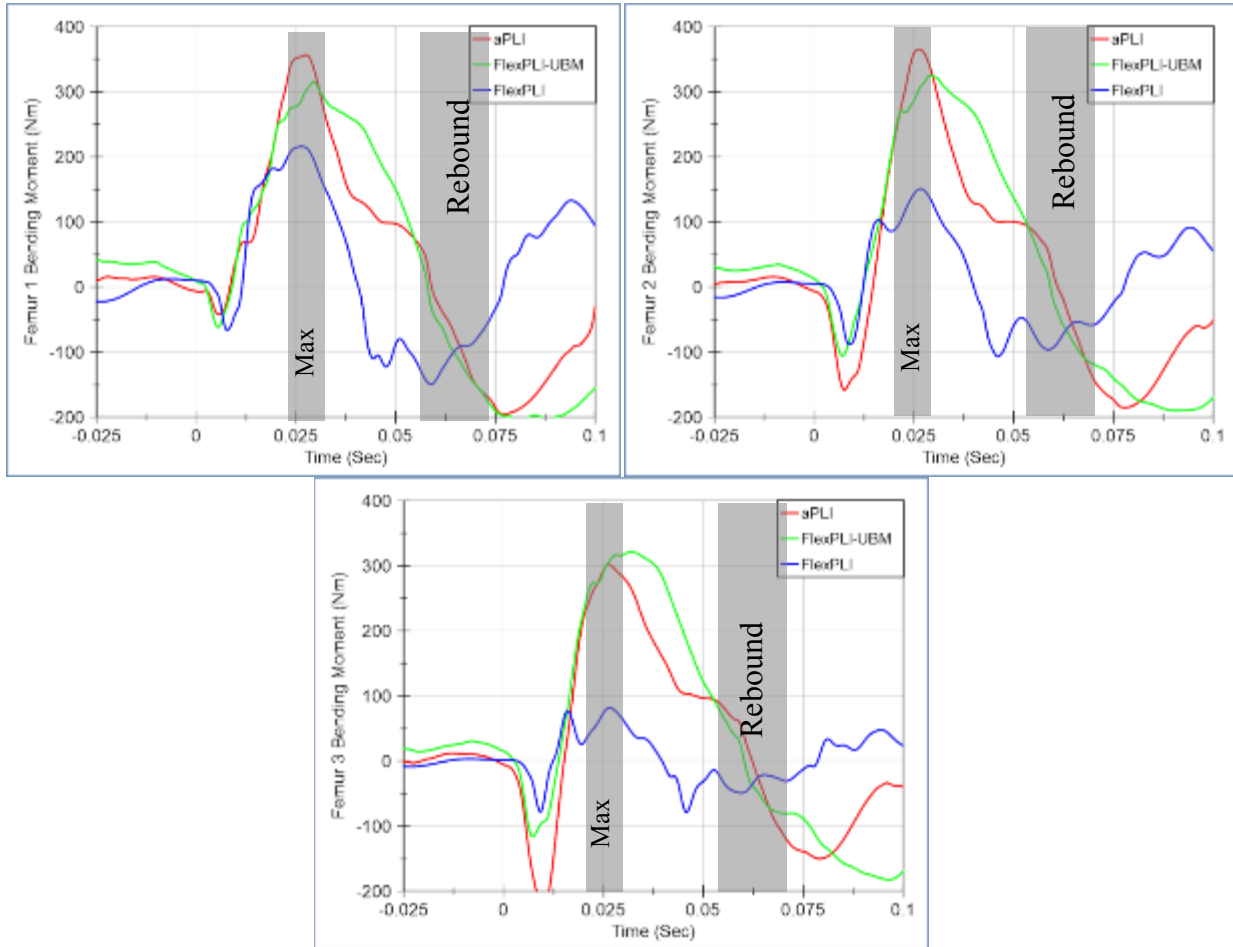


Figure 13. Femur bending moment time histories for the center impact: Femur 1 (closest to the knee) is shown at the top left; Femur 2 is at the top right; and Femur 3 (furthest from the knee) is at the bottom. The FlexPLI-UBM is shown in green ($T_{max} = 0.028$ s; $T_{Rebound} = 0.071$ s). The aPLI is shown in red ($T_{max} = 0.028$ s; $T_{Rebound} = 0.058$ s). The standard FlexPLI is shown in blue ($T_{max} = 0.022$ s; $T_{Rebound} = 0.053$ s). The grey areas indicate the regions of maximum bending and rebound, which correspond with the screen captures in Figure 12.

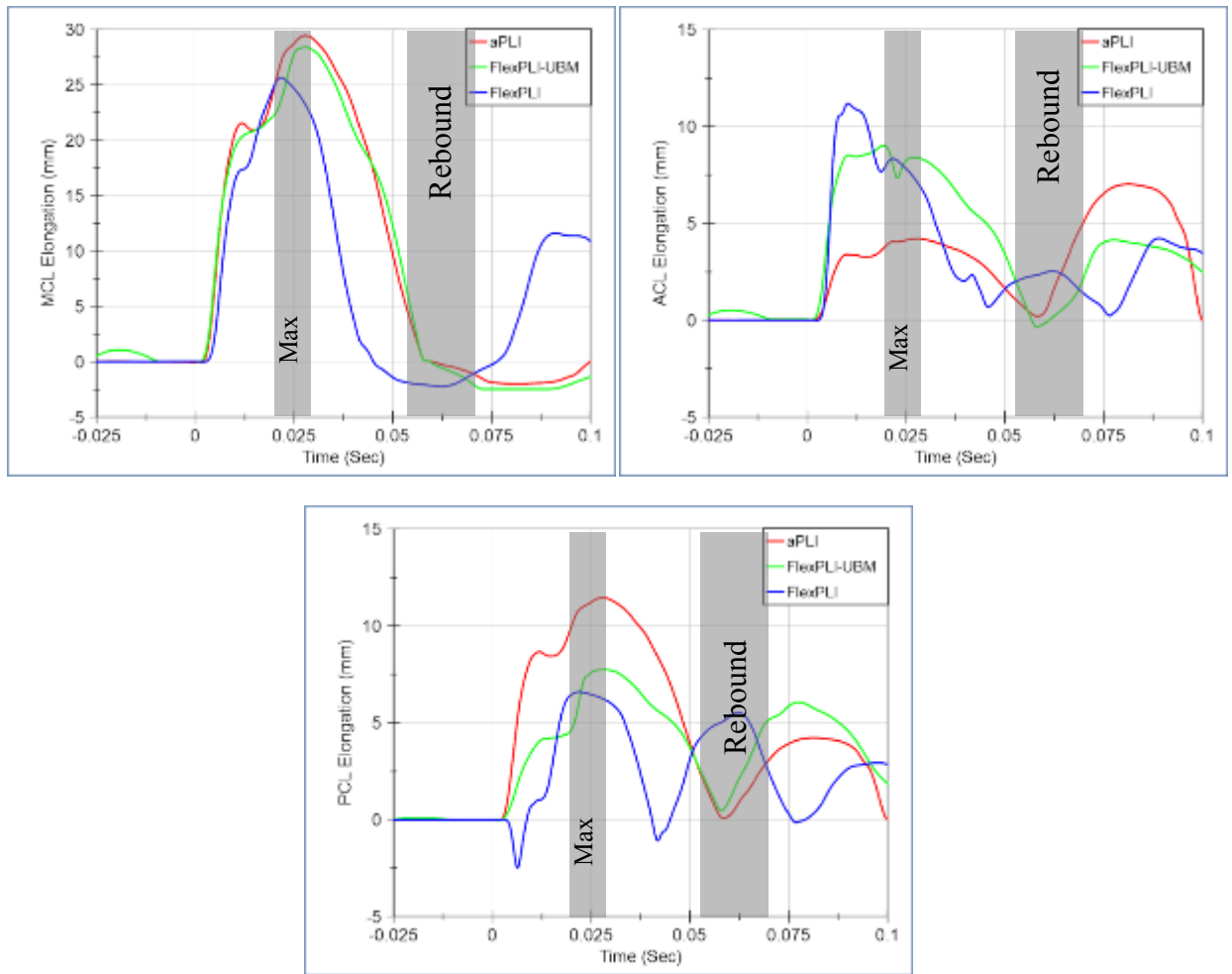


Figure 14. Ligament elongation time histories for the center impact: MCL is shown at the top left; PCL is at the top right; and ACL is at the bottom. The FlexPLI-UBM is shown in green ($T_{max} = 0.028$ s; $T_{Rebound} = 0.071$ s). The aPLI is shown in red ($T_{max} = 0.028$ s; $T_{Rebound} = 0.058$ s). The standard FlexPLI is shown in blue ($T_{max} = 0.022$ s; $T_{Rebound} = 0.053$ s). The grey areas indicate the regions of maximum bending and rebound, which correspond with the screen captures in Figure 12.

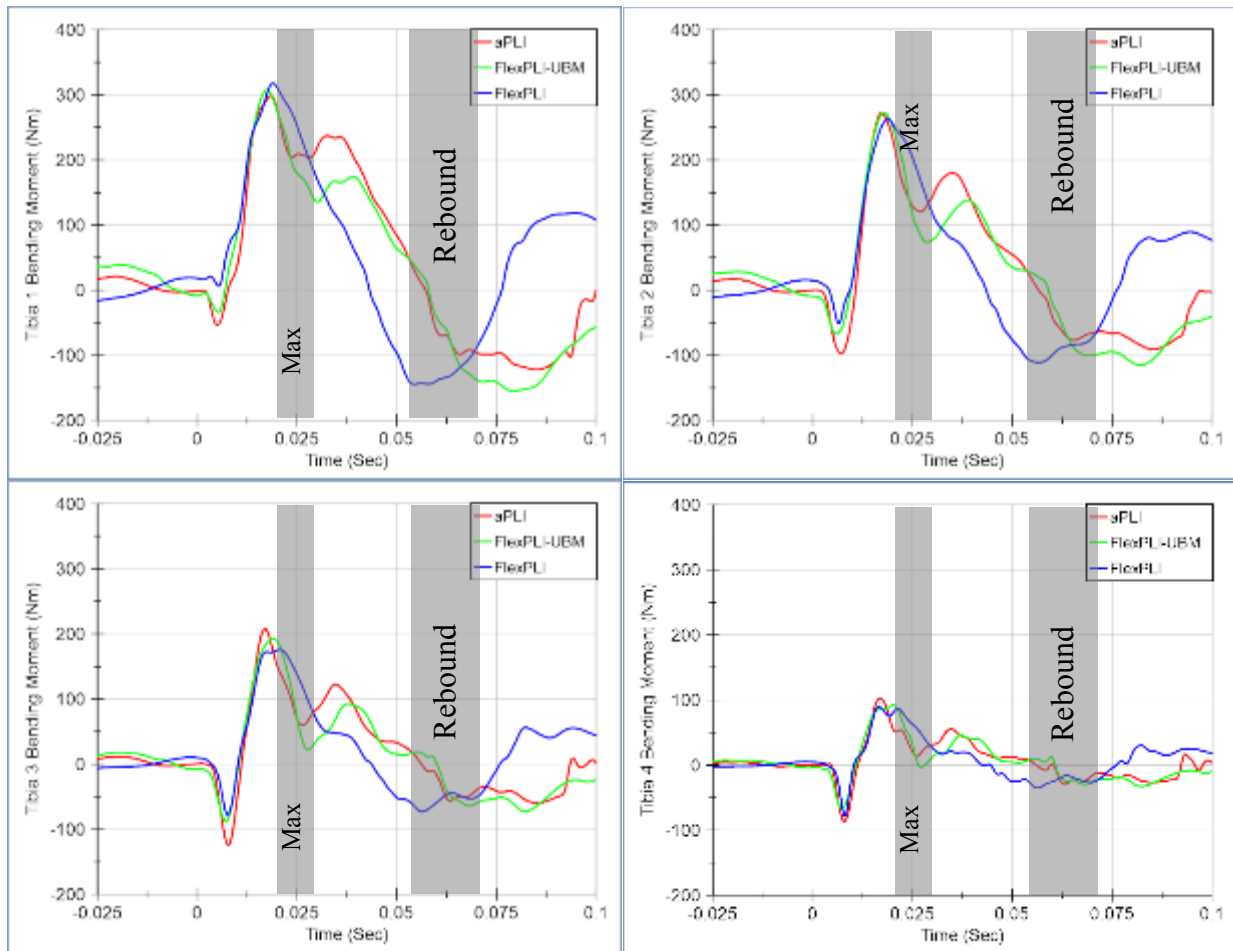


Figure 15. Tibia bending moment time histories for the center impact: Tibia 1 (closest to the knee) is shown at the top left; Tibia 2 is at the top right; Tibia 3 is at the bottom left; and Tibia 4 (furthest from the knee) is at the bottom right. The FlexPLI-UBM is shown in green ($T_{max} = 0.028$ s; $T_{Rebound} = 0.071$ s). The aPLI is shown in red ($T_{max} = 0.028$ s; $T_{Rebound} = 0.058$ s). The standard FlexPLI is shown in blue ($T_{max} = 0.022$ s; $T_{Rebound} = 0.053$ s). The grey areas indicate the regions of maximum bending and rebound, which correspond with the screen captures in Figure 12.

5.2. Outboard Impact Results

Screen captures from high speed videos of the FlexPLI-UBM, aPLI, and FlexPLI at time of first contact (T_0), time of maximum bending (T_{Max}), and time of rebound ($T_{Rebound}$) are shown in Figure 16 for the outboard impact. The three legforms show similar impact kinematics from time of first contact through time of maximum bending. The rebound phase is where the legforms deviate. The FlexPLI-UBM and aPLI maintain a forward pitch towards the vehicle during rebound while the FlexPLI pitches rearward and away from the vehicle. Additionally, there appears to be greater yaw rotation (z-axis rotation) in both the FlexPLI-UBM and FlexPLI than the aPLI.

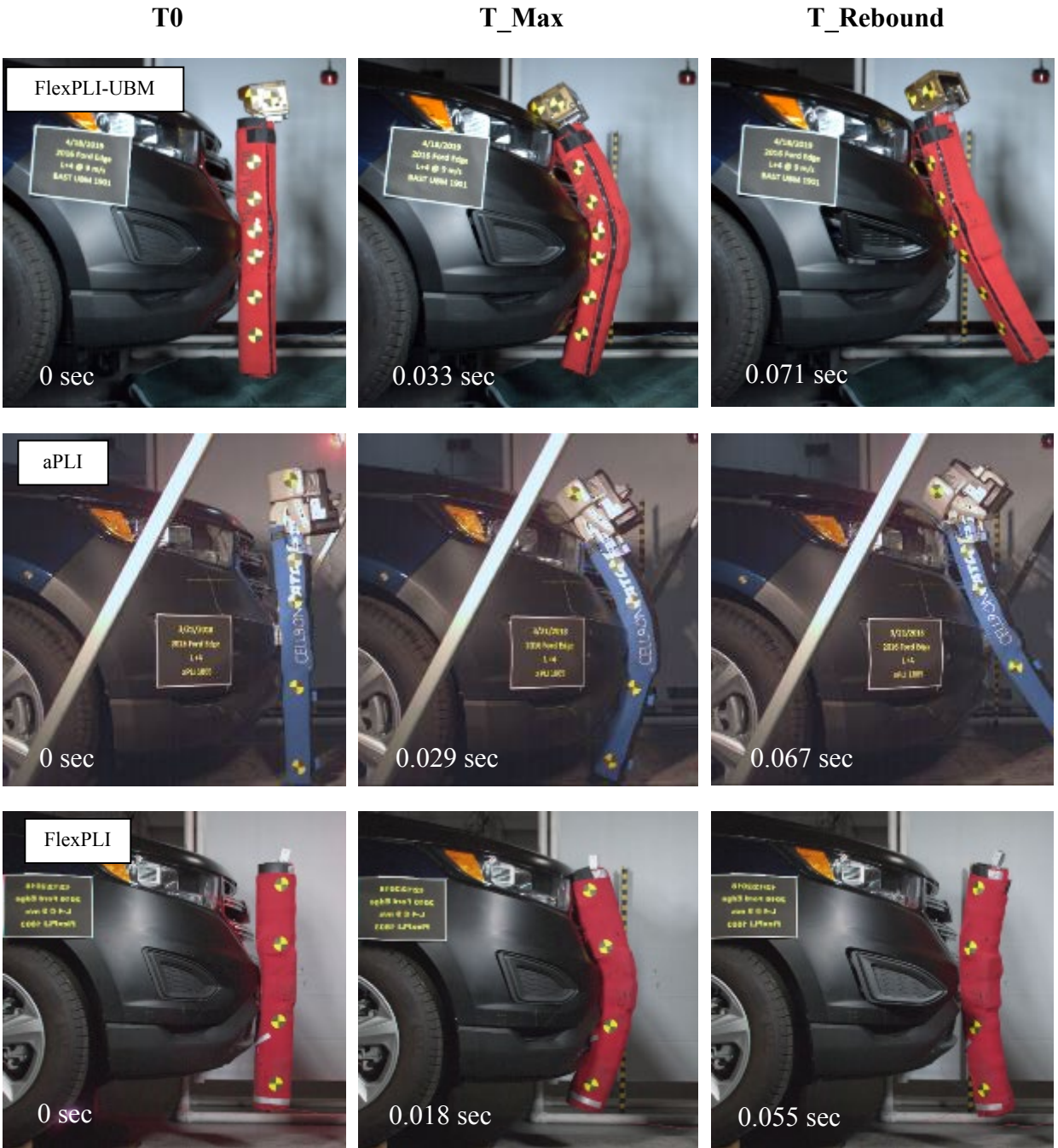


Figure 16. Outboard impact screen captures from high speed videos of the FlexPLI-UBM (Top Row), aPLI (Middle Row), and FlexPLI (Bottom Row) at time of first contact (T₀), time of maximum bending (T_{Max}), and time of rebound (T_{Rebound}).

Outboard impact time histories for femur bending moment (Figure 17), knee ligament elongation (Figure 18), and tibia bending moment (Figure 19) are shown below for the FlexPLI-UBM, aPLI, and FlexPLI. The results for the FlexPLI-UBM, aPLI, and FlexPLI are represented by the green, red, and blue curves, respectively. The results indicate that the advanced legforms exhibited greater femur bending moments and MCL/PCL elongations. The ACL elongation was much lower in the aPLI if looking at the magnitude of the initial peak. However, the aPLI exhibited a secondary peak after the time of maximum bending and during the rebound phase that was greater in magnitude than the first peak and comparable to the maximum elongations of the other two legforms. As with the center impact, the three legforms exhibited similar tibia bending moments.

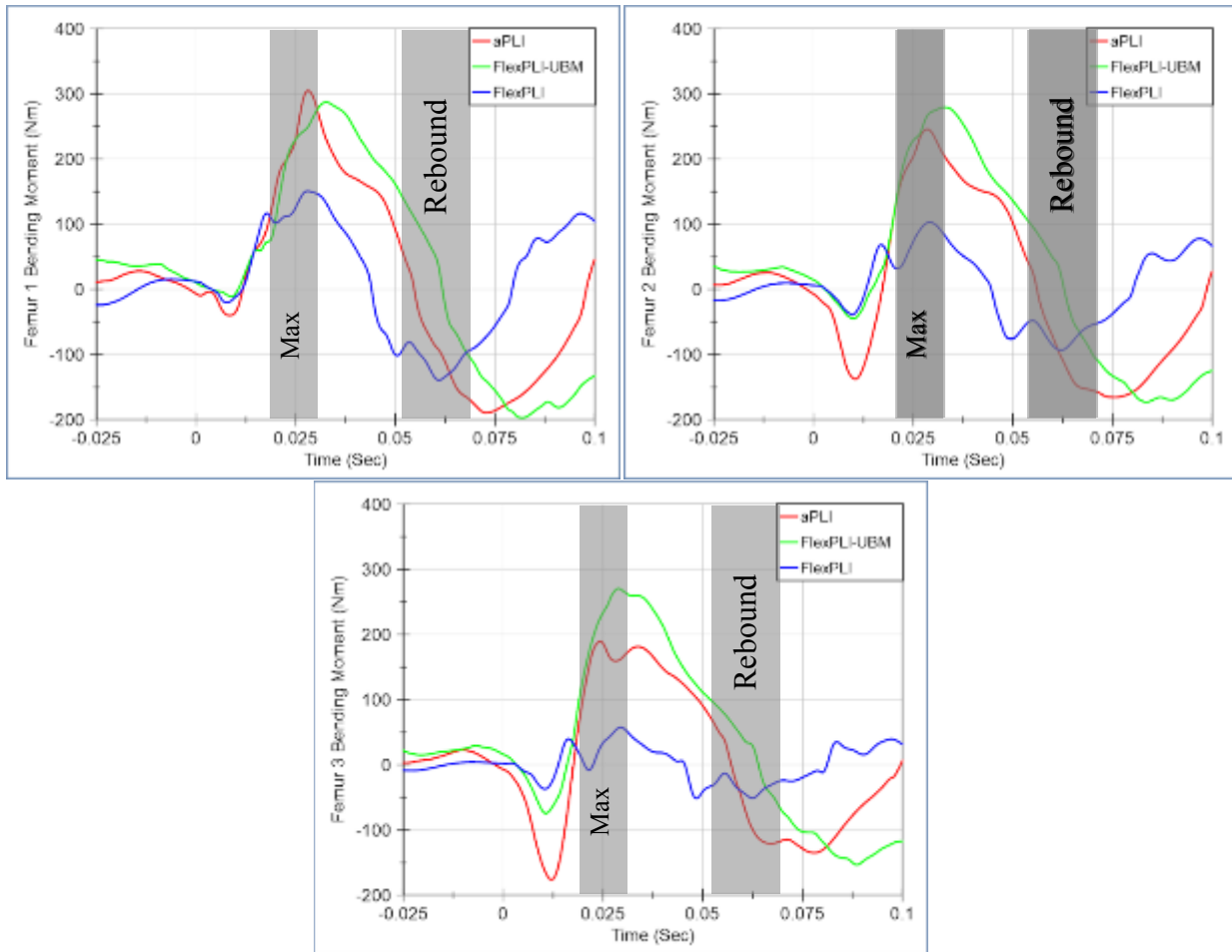


Figure 17. Femur bending moment time histories for the outboard impact: Femur 1 (closest to the knee) is shown at the top left; Femur 2 is at the top right; and Femur 3 (furthest from the knee) is at the bottom. The FlexPLI-UBM is shown in green ($T_{max} = 0.033$ s; $T_{Rebound} = 0.071$ s). The aPLI is shown in red ($T_{max} = 0.029$ s; $T_{Rebound} = 0.067$ s). The standard FlexPLI is shown in blue ($T_{max} = 0.018$ s; $T_{Rebound} = 0.055$ s). The grey areas indicate the regions of maximum bending and rebound, which correspond with the screen captures in Figure 16.

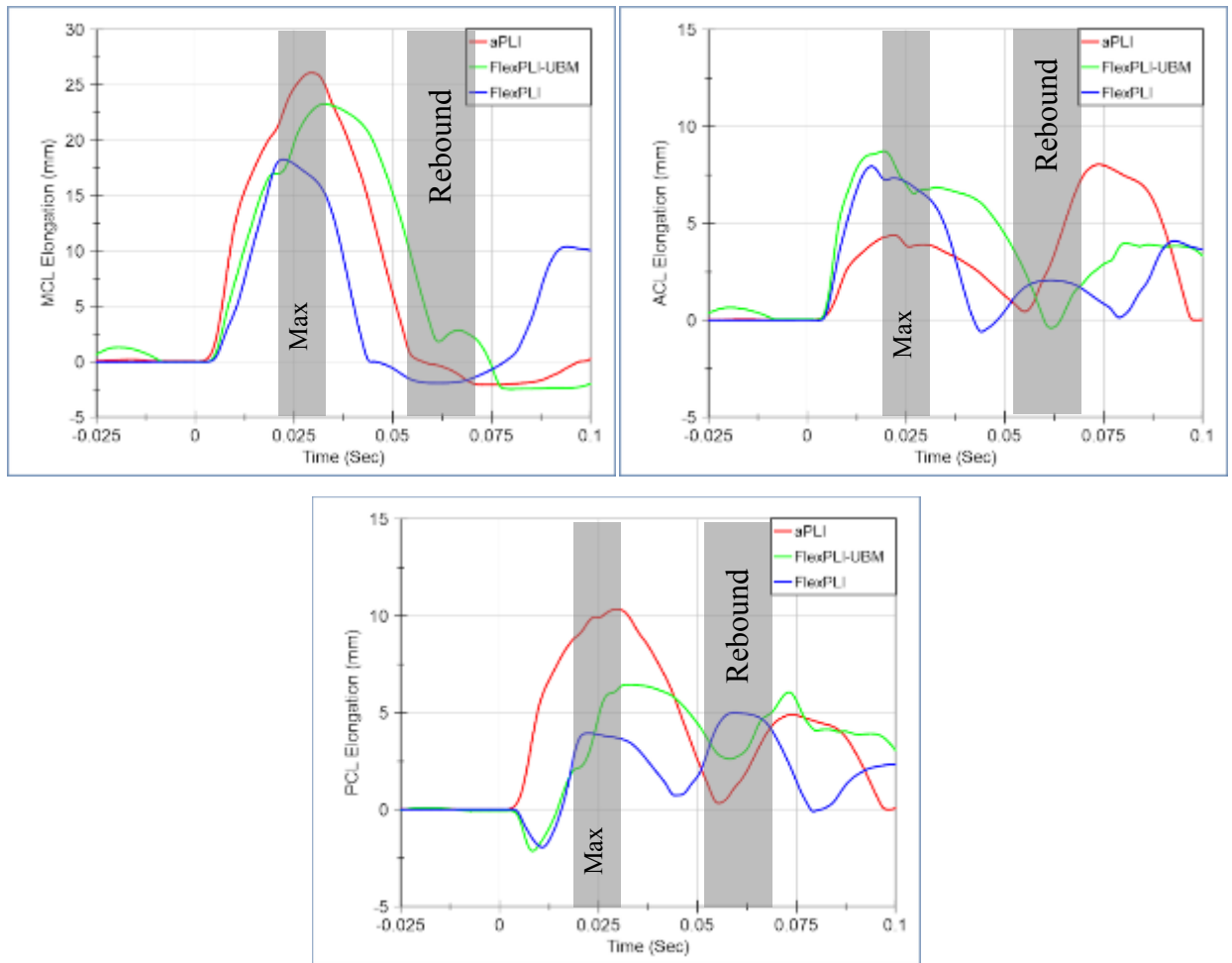


Figure 18. Ligament elongation time histories for the outboard impact: MCL is shown at the top left; PCL is at the top right; and ACL is at the bottom. The FlexPLI-UBM is shown in green ($T_{max} = 0.033$ s; $T_{Rebound} = 0.071$ s). The aPLI is shown in red ($T_{max} = 0.029$ s; $T_{Rebound} = 0.067$ s). The standard FlexPLI is shown in blue ($T_{max} = 0.018$ s; $T_{Rebound} = 0.055$ s). The grey areas indicate the regions of maximum bending and rebound, which correspond with the screen captures in Figure 16.

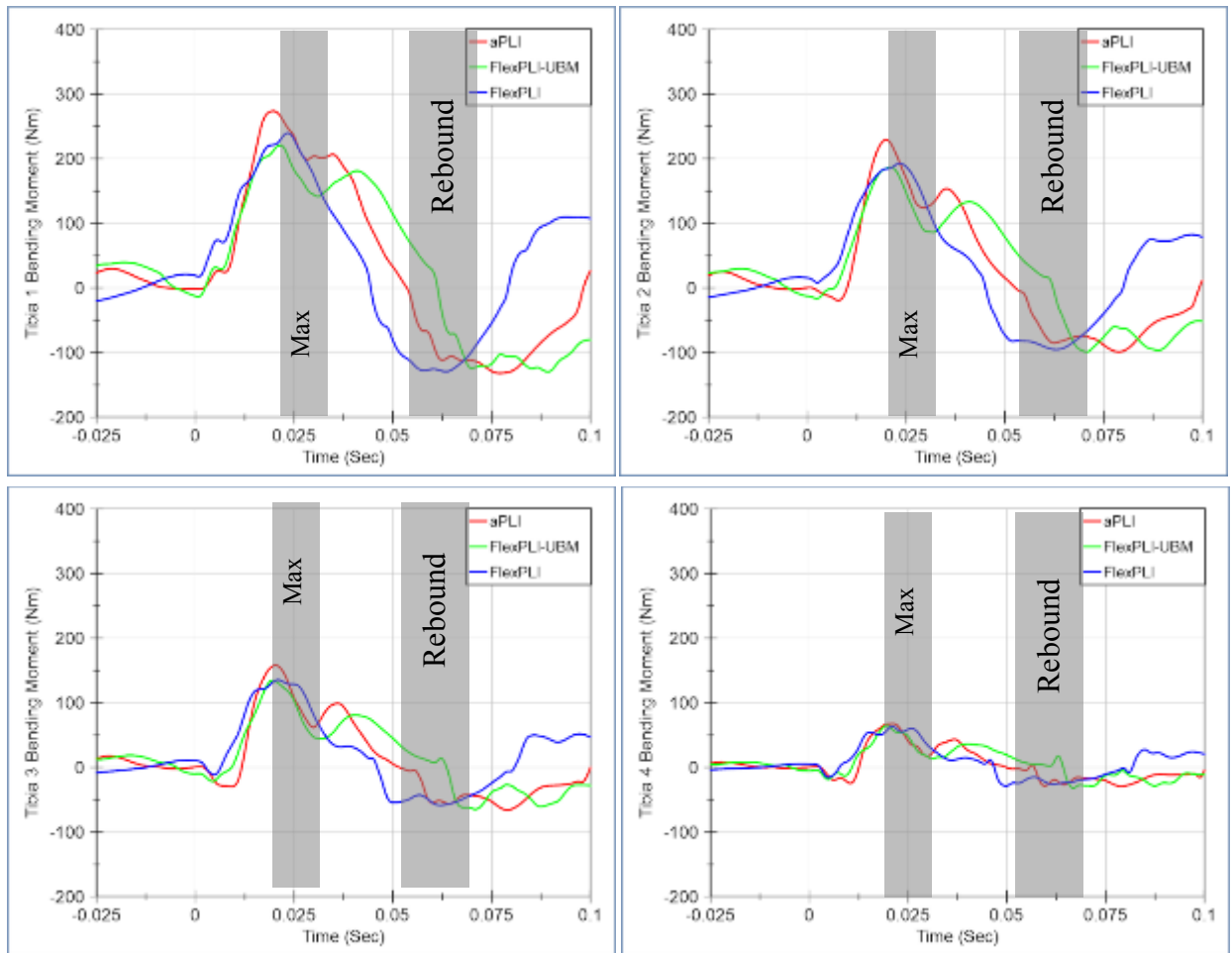


Figure 19. Tibia bending moment time histories for the outboard impact: Tibia 1 (closest to the knee) is shown at the top left; Tibia 2 is at the top right; Tibia 3 is at the bottom left; and Tibia 4 (furthest from the knee) is at the bottom right. The FlexPLI-UBM is shown in green ($T_{max} = 0.033$ s; $T_{Rebound} = 0.071$ s). The aPLI is shown in red ($T_{max} = 0.029$ s; $T_{Rebound} = 0.067$ s). The standard FlexPLI is shown in blue ($T_{max} = 0.018$ s; $T_{Rebound} = 0.055$ s). The grey areas indicate the regions of maximum bending and rebound, which correspond with the screen captures in Figure 16.

6. Summary

Table 2 presents the combined results of the three legforms tested at both the center and outboard impact locations. In general, when compared to the standard FlexPLI, the FlexPLI-UBM and aPLI both showed larger femur bending moments and larger MCL/PCL elongations while ACL elongations had mixed results. Additionally, the legform modifications and additional upper body mass were found to have little effect on the tibia bending moments as the three legforms showed similar values.

Table 2. Summary of peak magnitudes for the center and outboard impacts with the three legforms

	L0, Center			L ± 4, Outboard		
Legform	aPLI	UBM	FlexPLI	aPLI	UBM	FlexPLI
Test #	1807	1902	1804	1805	1901	1803
Femur Bending Moment (Nm)						
Femur 1	357	315	216	305	287	151
Femur 2	365	325	151	246	279	103
Femur 3	302	321	82	189	271	58
Knee Ligament Elongation (mm)						
MCL	29.4	28.4	25.7	26.1	23.3	18.3
ACL	4.2 (*7.0)	9.0	11.6	4.4 (*8.0)	8.7	8.2
PCL	11.4	7.7	6.3	10.3	6.4	4.7
Tibia Bending Moment (Nm)						
Tibia 1	299	308	318	274	221	240
Tibia 2	272	272	263	229	187	193
Tibia 3	208	192	176	158	135	136
Tibia 4	102	92	90	72	65	63

*Secondary peak value after maximum bending

7. Discussion

The FlexPLI lacks an upper body mass, which affects leg kinematics and the resulting femur measurements. For this reason, there are currently no proposed injury assessment values for the femur. The addition of an upper body mass to the legform raises its center-of-gravity (CG) location and, in order for this top-heavier version of the legform to display proper kinematics, the legform height with respect to the ground reference level was lowered for the FlexPLI-UBM and aPLI. Impact heights from the bottom of the legform to the ground reference level were reduced from 75 mm with the FlexPLI to 63 mm with the FlexPLI-UBM and 25 mm with the aPLI. Since the tibia lengths are the same between the three legforms, the varying impact heights at the same impact location caused the knees to interact with the vehicle bumper differently. For the three legforms, the knee centerline impact locations with respect to the Ford Edge front bumper are presented in Figure 20 below.



Figure 20. Knee centerline impact locations for the FlexPLI, FlexPLI-UBM, and aPLI.

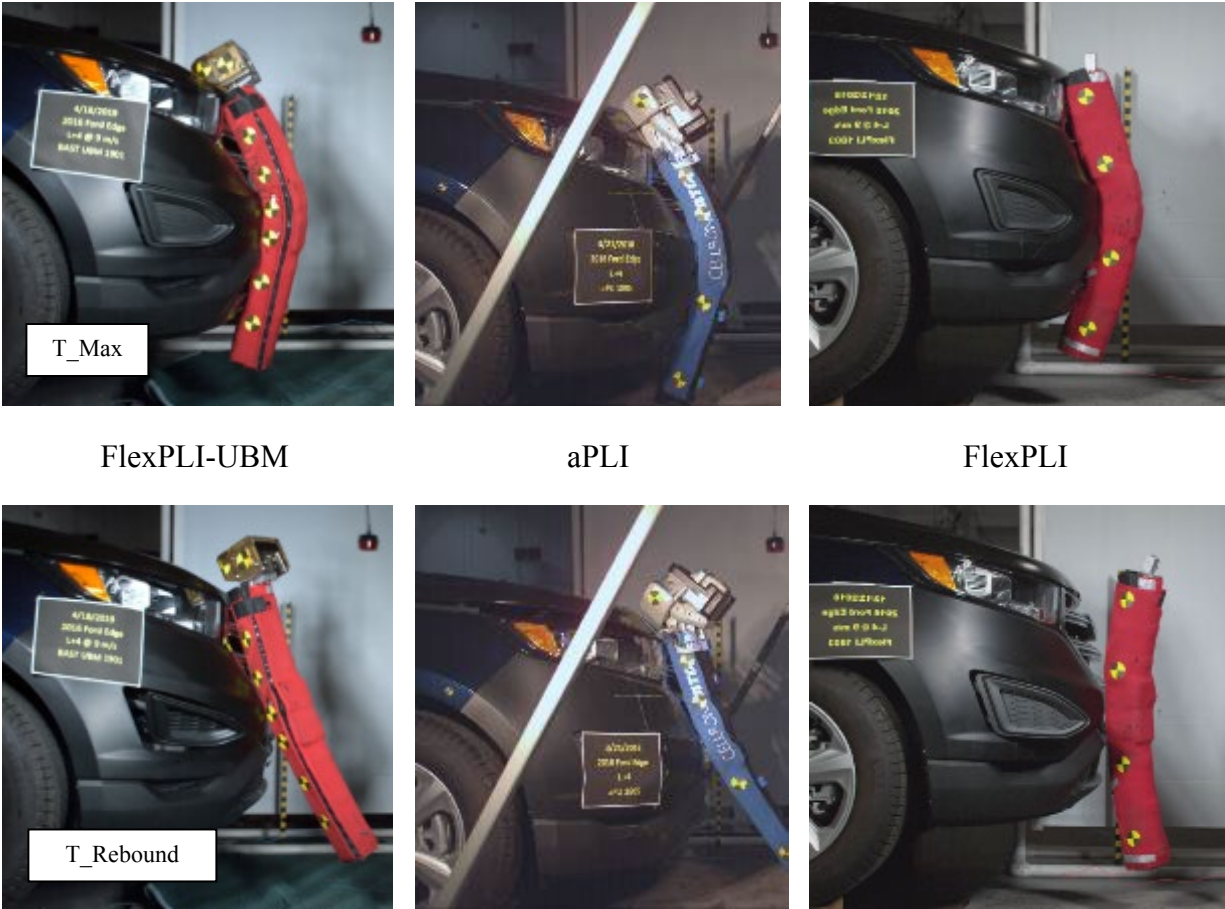
It was observed from this study that the addition of an upper body mass and the subsequent lower impact heights resulted in increased femur bending moments, even at lower impact speeds. However, it is unclear whether the increase in femur bending is due to the addition of the upper body mass, the change in impact height, or both. It is easy to understand how the addition of a mass to the top of the legform can produce greater bending moments in the femur. However, the knee and femur interactions with the vehicle front bumper can also have an effect. The knee centerline in the FlexPLI impact is closer to the top of the bumper beam area, which could allow for more rotation of the legform about the knee joint. In the FlexPLI-UBM and aPLI, the knee centerlines during impact are more towards the center and bottom of the bumper beam area, respectively, which could prevent knee joint rotation and produce more femur bending. Therefore, it is possible that even without the added upper body mass, as the knee centerline moves down along the bumper beam preventing knee joint rotation, femur bending moments can increase. More tests will need to be performed with the FlexPLI at the same impact heights of the FlexPLI-UBM and aPLI to better understand the effects of the added upper body mass and changes in impact height.

In general, at the time of maximum bending, the MCL and PCL ligament elongations were found to increase with the added upper body mass and lower impact heights while ACL elongations were mixed, with a large decrease in the aPLI and similar results between FlexPLI-UBM and FlexPLI. The increase in PCL and decrease in ACL elongations observed in the aPLI are likely due to the updated orientation of the ligaments as shown in Figure 7. With the ligaments oriented vertically and the PCL located medial to the ACL and further away from the impact side, the PCL can be expected to have a larger elongation than the ACL in the aPLI. The vertical ligament orientation also explains the larger secondary peak in the ACL during the rebound phase, since as the aPLI bends in the opposite (medial) direction, the ACL would be expected to stretch more than the PCL. In the FlexPLI-UBM, the PCL elongations were only slightly larger than the FlexPLI and the ACL elongations were generally similar. Since the FlexPLI-UBM and FlexPLI share the same ligament orientation, it can be expected that the two legforms would have similar PCL and ACL elongations with the slight differences being due to the upper body mass and impact height differences. The FlexPLI-UBM and FlexPLI exhibited greater ACL elongations than PCL elongations, opposite of the aPLI, which is also likely due to their ligament orientations. In the crossed orientation, as shown in Figure 7 for the FlexPLI-UBM and FlexPLI, it would be expected that the ACL would stretch more than the PCL during a lateral impact. More testing will need to be done to better understand and isolate the effects that added upper body mass, impact height differences, and ligament orientation have on ligament response.

The tibia bending moments seem to have remained the same for the three legforms suggesting that the upper body mass addition, resulting impact height changes, and different ligament orientation had no effect on the tibia response. This is a positive observation as the FlexPLI has been shown to be very accurate in evaluating below knee injury risk. However, this result may be vehicle specific and the tibia could respond differently to changes in impact height as the bumper beam height, front-end shape, and front-end stiffness varies between vehicles.

Furthermore, it should also be noted that both the FlexPLI-UBM and aPLI followed similar trends as the FlexPLI when comparing impact locations. For the three legforms, the center impacts were more severe than the outboard impacts, which was also the case in standard 11.1 m/s impacts with the FlexPLI to the 2016 Ford Edge (Suntay & Stammen, July 2019).

Looking at the impact kinematics, the legforms with added upper body mass were found to be different than the standard FlexPLI. At both center and outboard impact locations, all three legforms showed similar kinematics from time of first contact with the vehicle through the time of maximum bending of the legforms. Legform kinematics begin to deviate from the time of maximum bending and throughout the rebound phase. During this time, the FlexPLI pitches rearward and away from the vehicle while the upper portions of both the FlexPLI-UBM and aPLI remain in contact with the vehicle longer as shown in Figure 21, which more closely matches the kinematics of full-body model simulations (Issiki et al., 2018; Zander et al., 2019).



T_Max

FlexPLI-UBM

aPLI

FlexPLI

T_Rebound

Figure 21. Outboard impact screen captures from high speed videos at T_Max (Top Row), and T_Rebound (Bottom Row) for the FlexPLI-UBM (left), aPLI (center), and standard FlexPLI (right).

Lastly, there also appears to be a significant amount of yaw rotation (z-axis rotation) in the FlexPLI-UBM and standard FlexPLI at this outboard impact location that is not seen in the aPLI. This is likely due to the design of the knee blocks. Both the standard FlexPLI and FlexPLI-UBM have square-edged knee blocks, which would cause the legform to rotate when contacting a curved surface. In contrast, the aPLI was designed with a rounded knee block (Figure 6) with the intention of improving consistency with human body model kinematics in oblique impacts. Contact between the aPLI's rounded knee block and curved outboard bumper profiles, in addition to the revised moment of inertia about the z-axis, resulted in less rotation of the legform to be more comparable with human body model kinematics (Zander et al., 2019).

8. Limitations

Although only a few lower speed tests to a single vehicle were performed in this study, a good preliminary look at both the FlexPLI-UBM and aPLI was achieved. However, each of the three legforms were tested at different specified heights and not enough tests were performed to fully understand how the design updates affect legform response. Due to the differing impact heights, these tests were not able to isolate the influences of upper body mass and resulting CG location, legform height and resulting knee-to-bumper interaction, and cruciate ligament orientation. Tests in this study were also performed on a single, higher bumper sport utility vehicle and legform responses might be different for vehicles with different front-end heights, shapes, and stiffness. Lastly, tests in this study were performed at 9 m/s instead of the specified 11.1 m/s. Although it is expected that the response trends of the three legforms will be similar at a higher impact speed, there is a possibility that a higher speed could affect their response differently.

9. Conclusion

Overall, both the FlexPLI-UBM and aPLI were easy to use and adapt to VRTC's launch system. A major positive feature of the FlexPLI-UBM is that the upper body part is a bolt-on attachment to the existing FlexPLI with a manageable weight. One downside with the FlexPLI-UBM tested in this study is that its upper body part lacks instrumentation. Although the aPLI was much heavier, it did consist of additional instrumentation in its upper body part as well as an improved biofidelic design, which proved to influence rotational kinematics in non-perpendicular impacts.

Preliminary test results with both the FlexPLI-UBM and aPLI showed increased femur bending moments, increased MCL and PCL elongations, and more realistic impact kinematics as compared to the standard FlexPLI. Both legforms also showed similar trends as the FlexPLI when comparing results at the same impact location on the same vehicle. Additionally, the tibia bending moments were similar for the three legforms suggesting that the upper body mass addition, resulting impact height changes, and different ligament orientation had no effect on the tibia response. This is a positive observation as the current FlexPLI has been shown to be a very good instrument for its present application in Euro NCAP and ECE No. 127 where it is used in evaluating below knee injury risk.

10. References

- Isshiki, T., Antona-Makoshi, J., Konosu, A., & Takahashi, Y. (2018, September 12-14). *Consolidated technical specifications for the advanced pedestrian legform impactor (aPLI)* (Report No. IRC-18-42). 2018 International Research Council on the Biomechanics of Injury (IRCOBI) Conference, Athens, Greece.
- Miyazaki, H., Matsuoka, F., Kuwahara, M., Kitagawa, Y., & Yasuki, T. (2009, June 15-18). *Development of flexible pedestrian legform impactor FE model and comparative study with leg behavior of human FE model THUMS* (Report No. 09-0112). 21st International Technical Conference on the Enhanced Safety of Vehicles (ESV), Stuttgart, Germany.
- Suntay, B., & Stammen, J. (2014, May). *Technical evaluation of the flexible pedestrian legform impactor (Flex-PLI)* (Report No. NHTSA 2008-0145 in NHTSA Docket NHTSA-2019-0112-0003). National Highway Traffic Safety Administration.
https://downloads.regulations.gov/NHTSA-2019-0112-0003/attachment_1.pdf
- Suntay, B., & Stammen, J. (2019, May). *Technical evaluation of the TRL pedestrian upper legform* (Report No. DOT HS 812 659). National Highway Traffic Safety Administration. www.regulations.gov/document?D=NHTSA-2019-0112-0007
- Suntay, B., Stammen, J., & Martin, P. (2019, June). *Pedestrian protection – Assessment of the U.S. vehicle fleet* (Report No. DOT HS 812 723). National Highway Traffic Safety Administration. Available at www.regulations.gov/document?D=NHTSA-2019-0112-0005
- Zander, O., & Hynd, D. (2018, May 28). *Draft test and assessment procedure for current and advanced passive safety systems (4.1a) and draft test and assessment procedures for current and advanced passive VRU safety systems (4.1b)*. SENIORS [acronym for Safety Enhanced Innovations for Older Road Users].
<https://ec.europa.eu/research/participants/documents/downloadPublic?documentIds=080166e5bb161be9&appId=PPGMS>
- Zander, O., Wisch, M., Ott, J., Burleigh, M., Peldschus, S., & Hynd, D. (2019, September 11-13). *Development and evaluation of an upper body mass (UBM) for the flexible pedestrian legform impactor (FlexPLI) and for incorporation within improved test and assessment procedures—Results from SENIORS* (Report No. IRC-19-54). 2019 International Research Council on the Biomechanics of Injury (IRCOBI) Conference, Florence, Italy.

DOT HS 813 086
February 2022



U.S. Department
of Transportation
**National Highway
Traffic Safety
Administration**

